RSC Advances

ROYAL SOCIETY OF CHEMISTRY

www.rsc.org/advances

RSC Advances RSCPublishing

COMMUNICATION

Copper-Templated Synthesis of Gold Microcages for Sensitive Surface-Enhanced Raman Scattering Activity

Cite this: DOI: 10.1039/x0xx00000x

Chuncai Kong, Jian Lv, Shaodong Sun, Xiaoping Song, Zhimao Yang*

Received 00th January 2012,
Accepted 00th January 2012

DOI: 10.1039/x0xx00000x
www.rsc.org/

We have demonstrated a facile Cu-templated approach for synthesis of nanoparticle-aggregated hollow gold microcages. The as-prepared gold microcages as an active substrates exhibit remarkable surface-enhanced Raman scattering (SERS) activity for 4-mercaptobenzoic acid (4-MBA).

Surface-enhanced Raman spectroscopy (SERS) has been attracting significant attentions since its discovery in the 1970s.[1] It is now an powerful technique in chemical and biological analyses at the single molecule level because of its stability, sensitivity and anti-interference.[2] Up to now, numerous noble metals has been synthesized as the active substrates of SERS, including Au flowers,[3] Au nanopatches, [4] porous Ag,[5] Au-Ag nanocages,[6] Ag@Pd nanocrystals, [7] aggregates of Au nanoparticles [8] and polymer – Au hybrid,[9] et. al. Both experimental measurements and theoretical simulation have shown that the SERS enhancement mostly depended on the substrate features, including the size, shape and composition.[3, 10] "Hot spots", which is the enhanced electromagnetic fields, are essential for the sensitive SERS substrate. On the surface of nanoparticles-aggregated hollow structures, there are usually many nanogaps and protuberances which can provide high density of"hot spots", [3, 5, 11] leading to a high performance on SERS.

Hollow Au micro/nanostructures have been widely applied in sensing,[12] catalysis, [13] and biomedical therapy,[14] due to their chemical stability and good biocompatibility. Compared with these solid structures, the hollow ones are attractive because of their high specific surface areas, low densities, hollow interiors and low-cost.[15] Furthermore, the surface morphology which is crucial for the SERS performance. Thus, the design and synthesis of hollow Au architectures through a lower cost and facile synthetic method is still needed.

Galvanic replacement reaction, as a simple and effective method, has been widely used to produce nanomaterials with various mophologies. The structure and morphology of the final hollow structures can be accurately controlled by manipulating the reaction conditions in the galvanic diplacement reaction with micro/nanoparticles as sacrificial templates. Our group have prepared cauliflower-like and paddy-like copper nanostructures using zinc foil as reductant.[16] Yang reported the synthesis of noble metal alloy mesocages with Cu_2O as sacrificial templates.[17] Xia et al. obtained Au nanocages by using Ag nanocubes as templates. [18] But there are few reports about the synthesis of Au hollow structures with Cu as the sacrificial template. Lu and co-workers got Au nanotubes by using $HAuCl_4$ with Cu nanowires. [19] And in another example, Xie reported that Au_xCu_{1-x} nanocages and nanotubes could be formed by galvanic replacement between Cu nanostructures and $HAuCl_4$. [20]

The potential difference provides the dynamic of the galvanic replacement reaction. According to the contrast of the cell potentials, the standard reduction potential $E^{\theta}(Cu^{2+}/Cu) = +0.342$ V (vs SHE) is lower than $E^{\theta}(AuCl_4^-/Au) = +0.99$ V. [18b] Therefore, the Au can be easily reduced by Cu templates. Herein, we present the synthesis of Au microcages through the galvanic replacement reaction between hollow Cu microcages and $HAuCl_4$ aquesous solution. The as-prepared Au microcages displayed good SERS activity for 4-mercaptobenzoic acid (4-MBA) due to the protuberances and nanogaps between the neighboring nanoparticles..

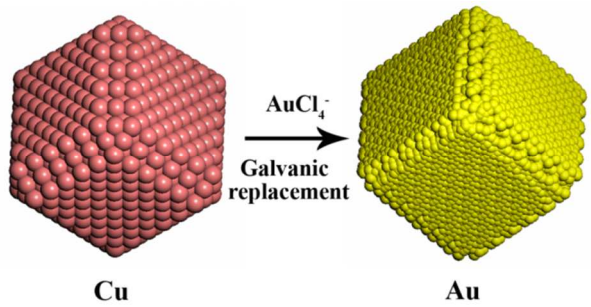

Scheme 1 A schematic illustration of the synthesis for hollow Au microcages using hollow Cu templates

Our strategy to achieve the hollow Au microcages is based on a reduction/etching route. It can be synthesized by a two-step process, *i.e.* the formation of hollow Cu architectures *via* a Cu_2O-templated solution route (see Fig. S1), then the sacrifice on hollow Cu templates by a facile galvanic replacement reaction (see Scheme 1). In a typical synthesis, 3.84 mg of the as-prepared hollow Cu microstructures were dispersed in 15 ml deionized water which contained 0.05g PVP in a conical flask. 2 mL of $HAuCl_4$

aqueous solution (20 mM) was added dropwise after the mixture was stirred for 10 min. Finally, a wine solution was obtained after the reaction running for 30 min at room temperature. Then the product was cleaned with deionized water and ethanol by repeated centrifugation. And the final product was dried at 50 ℃ in a vacuum drying oven for further characterization and mearsurement.

SERS of the as-prepared products were acquired using an HR 800 Raman spectrometer (HORIBA JOBIN YVON) with a CCD detector and He-Ne laser (633 nm). The SERS spectra were collected at 100x objective and an accumulation time of 20 s. In addition, the grating was 600 g mm^{-1} and the filter in the SERS spectra was D1. The as-prepared Au hollow microcagees were added into 1 ml of 4-mercaptobenzoic acid ethanol solution with different concentration. The solutions were sonicated for 3 min and left undisturbed for another 2 h, 20 μl of the solution droped on a glass subtrate and then dried for SERS measurements.

Hollow Au microcages were obtained by a galvanic replacement reaction approach, using $HAuCl_4$ as the Au source and hollow Cu microcages as the reductant. Fig. S2a shows the XRD pattern of as-prepared product, and the sharp peaks at 38.3°, 44.5°, 64.7° and 77.7° are indexed to the diffraction from the (111), (200), (220) and (311) of face-centered cubic (fcc) Au (JCPDS file No.65-8601). No peaks of impurities are detected, suggesting the high purity of the as-obtained Au microcages. The purity and the composition of the as-prepared Au microcages were further investigated by XPS. As shown in Fig.S2b, the peaks located at 83.6 eV and 87.2 eV are respectively assigned to core-level Au $4f_{7/2}$ and Au $4f_{5/2}$, corresponding to those of Au^0.[21] The morphology and structure were investigated by FESEM and TEM. As shown in Fig.1a, the Au microcages are well monodisperse and have an average size of 2.3±0.3 μm (Fig. S3a). Inset of Fig. 1a dispalys the SEM image of a broken Au microcage particle, which suggesting that the product has a hollow interior. Fig. 1b and c show that the Au microcage is consist of numerous small particles with the average size of 42.2±7.5 nm (Fig. S3b). The raised particles on the surface would enhance the SERS activity. The hollow interior and rough surface were further observed by TEM images (as shown in Fig. 1d and Fig. 1e). The lattice spacing shown in HRTEM image (Fig. 1f) is 0.236 nm which is well agreement with the (111) of Au. Fig. S4 shows the Uv-vis spectra of Au microcages and that after addition of 4-MBA. The spectra are dominated by the surface plasmon resonance of the Au microcages, and there is no observable change after addition of 4-MBA.

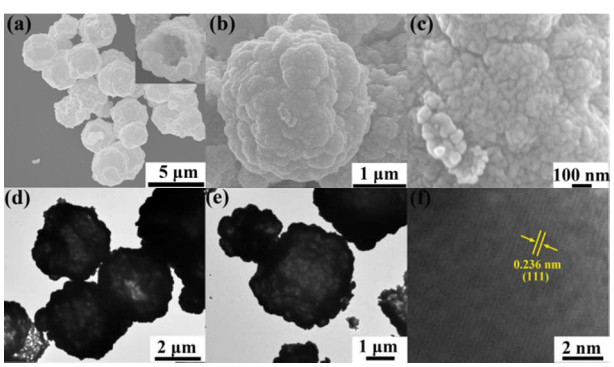

Fig. 1 Typical images of as-prepared Au microcagees: (a) low-magnification, (b) individual particle and (c) high-magnification FESEM images; inset of (a) is FESEM image of a broken particle (d) low-magnification, (e) individual particle and and (f) high-magnification TEM and HRTEM images, inset is the FFT of (f).

4-mercaptobenzoic (4-MBA) was selected as the probe molecules to study the SERS activity of as-prepared Au microcagees. SERS spectra of 4-MBA with different concentrations adsorbed on Au microcagees are shown in Fig. 2, which are similar with previous report.[11, 22] The intrinsic peaks observed at about 1078 cm^{-1} and 1589 cm^{-1} are attribuded to ν_{8a} and ν_{12} aromatic ring vibrations, respectively.[11, 23 24] There are some shift for the SERS spectrum between solid 4-MBA and 4-MBA on Au microcages, suggesting a strong interaction with the Au surface.[25] Fig. S5 shows the linear relationship between the intensities at 1589 cm^{-1} and the logarithmic concentration of 4-MBA. The Raman intensities vary linearly with the concentration of 4-MBA in the range of 10^{-7} to 10^{-4} M with a correlation factor of 0.985. And this linear plot provides a calibration for the quantitative detection of 4-MBA. The SERS enhancement factor (EF) was estimated based on the following equation to further evaluate the enhancement ability of the Au microcages.[4, 23]

$$EF = (I_{SERS}/N_{SERS})/(I_{bulk}/N_{bulk})$$

Where I_{SERS} and I_{bulk} are the Raman scanttering intensity of 4-MBA on the surface of Au microcages and the normal spectra of the bulk 4-MBA, respectively. And N_{SERS} and N_{bulk} are the number of 4-MBA molecules under the detecting spot (1×1 μm^2) for the Au sample and bulk, respectively. The measured Raman scattering intensity for 10^{-4} M, 10^{-5} M, 10^{-6} M and bulk 4-MBA at 1589 cm^{-1} are 25222, 15342, 11858 and 1183, respectively. According to the penetration depth of the focused laser (13 μm) and the bulk density of 4-MBA (1.5 g cm^{-3}), $N_{bulk} = 1.13\times10^{11}$. The number density of nanoparticles is about 410 μm^{-2}. For the 10^{-4} M of 4-MBA, the packing density absorbed on the surface is ~3.01×10^5 molecules per μm^{-2}.[21, 26] So the $N_{SERS} = 3.4\times10^5$, and the EF was then calculated to be 7.1×10^6 based on the peak at 1589 cm^{-1}. By the same method, the EF are estimated to be 4.31×10^6 and 3.33×10^6 for 10^{-5} M and 10^{-6} M of 4-MBA, respectively. The obtained EF are comparable to that of other Au nanostructure.[27]

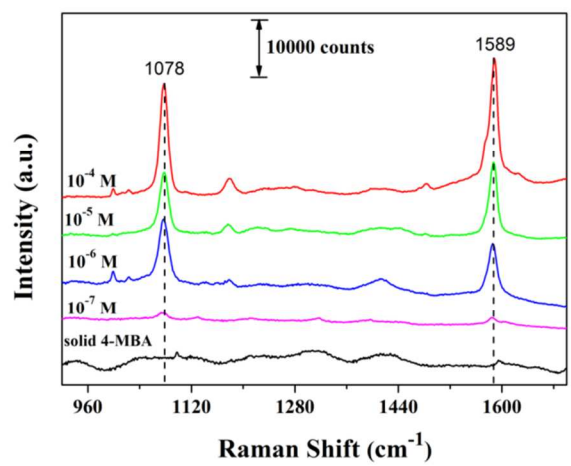

Fig. 2 Raman spectrum of solid 4-MBA and SERS spectra of 4-MBA with different concentrations adsorbed on Au microcages

Conclusions

In summary, we have successfully synthesized nanoparticle-aggregated Au microcages by using hollow Cu microstructures as the sacrificial templates. The SERS activity of Au microcages as substrates were further evaluated by using 4-MBA as the probe molecules. The EF was up to the order of 10^6,

indicating that the Au microcage is a promising SERS substrates for sensor detection.

Acknowledgment

This work was supported by National Science Foundation of China (NSFC No. 51272209 and 51302213), Doctoral Fund of Ministry of Education of China (No. 20120201120051), Program for Key Science and Technology Innovative Team of Shaanxi Province (No. 2013KCT-05), Youth Foundation of Shaanxi Province of China (No. 2012JQ6007), and Fundamental Research Funds for the Central Universities of China.

Notes and references

School of Science, Key Laboratory of Shannxi for Advanced Materials and Mesoscopic Physics, State Key Laboratory for Mechanical Behavior of Materials, Xi'an Jiaotong University, Collaborative Innovation Center of Suzhou Nano Science and Technology, Xi'an 710049, ShaanXi, People's Republic of China.. E-mail: zmyang@mail.xjtu.edu.cn

Electronic Supplementary Information (ESI) available: XRD pattern and FESEM images of Cu_2O and the hollow Cu, XRD pattern, XPS spectrum, size distribution and Uv-vis spectra of the as-prepared Au microcages. The linear relationship between the intensities at 1589 cm^{-1} and the logarithmic concentration of 4-MBA. See DOI: 10.1039/b000000x/

1 (a) M. Fleischmann, P. J. Hendra and A. J. McQuillan, *Chem. Phys. Lett.,* 1974, 26, 163-166; (b) D. L. Jeanmaire and R. P. Van Duyne, *J. Electroanal. Chem. Interfacial Electrochem.*, 1977, **84**, 1-20.

2 M. D. Porter, R. J. Lipert, L. M. Siperko, G. F. Wang and R. Narayanan, *Chem. Soc. Rev.*, 2008, **37**, 1001-1011.

3 M. Pradhan, J. Chowdhury, S. Sarkar, A. K. Sinha and T. Pal, *J. Phys. Chem. C*, 2012, **116**, 24301-24313.

4 J. He, P. Zhang, J. L. Gong and Z. H. Nie, *Chem. Commun.*, 2012, **48**, 7344-7346.

5 X. Luo, S. M. Lian, L. Q. Wang, S. C. Yang, Z. M. Yang, B. J. Ding and X. P. Song, *CrystEngComm*, 2013, **15**, 2588-2591.

6 M. Rycenga, K. K. Hou, C. M. Cobley, A. G. Schwartz, P. H. C. Camargo and Y. N. Xia, *Phys. Chem. Chem. Phys.*, 2009, **11**, 5903-5908.

7 L. F. Zhang and C. Y. Zhang, *Nanoscale*, 2013, 5, 6074-6080.

8 I. Blakey, Z. Merican and K. J. Thurecht, *Langmuir*, 2013, **29**, 8266-8274.

9 (a) P. Dey, I. Blakey, K. J. Thurecht and P. M. Fredericks, *Langmuir,* 2014, 30, 2249-2258; (b) P. Dey, I. Blakey, K. J. Thurecht and P. M. Fredericks, *Langmuir*, 2012, **29**, 525-533.

10 M. A. Mahmoud, *Langmuir*, 2013, **29**, 6253-6261.

11 S. W. Li, P. Xu, Z. Q. Ren, B. Zhang, Y. C. Du, X. J. Han, N. H. Mack and H. L. Wang, *ACS App. Mate. Interfaces*, 2012, **5**, 49-54.

12 M. A. Mahmoud and M. A. El-Sayed, *J. Am. Chem. Soc.*, 2010, **132**, 12704-12710.

13 X. W. Liu, *RSC Adv.*, 2011, **1**, 1119-1125.

14 (a) J. B. Song, J. J. Zhou and H. W. Duan, *J. Am. Chem. Soc.*, 2012, **134**, 13458-13469; (b) S. E Skrabalak, J. Y. Chen, L. Au, X. M. Lu, X. D. Li and Y. N. Xia, *Adv. Mater.*, 2007, **19**, 3177-3184.

15 X. W. Lou, L. A. Archer and Z. C. Yang, *Adv. Mater.*, 2008, **20**, 3987-4019.

16 (a) C. C. Kong, S. D. Sun, J. Zhang, H. D. Zhao, X. P. Song and Z. M. Yang, *CrystEngComm*, 2012, **14**, 5737-5740; (b) S. D. Sun, C. C. Kong, L. Q. Wang, S. C. Yang, X. P. Song, B. J. Ding and Z. M. Yang, *CrystEngComm*, 2011, **13**, 1916-1921.

17 F. Hong, S. D. Sun, H. J. You, S. C. Yang, J. X. Fang, S. W. Guo, Z. M. Yang, B. J. Ding and X. P. Song, *Cryst. Growth Deg.*, 2011, **11**, 3694-3697.

18 (a) S. E. Skrabalak, J. Y. Chen, Y. G. Sun, X. M. Lu, L. Au, C. M. Cobley and Y. N. Xia, *Accounts Chem. Res.*, 2008, **41**, 1587-1595; (b) L. Au, X. M. Lu and Y. N. Xia, *Adv. Mater.*, 2008, **20**, 2517-2522.

19 X. F. Lu, M. McKiernan, Z. M. Peng, E. P. Lee, H. Yang and Y. N. Xia, *Sci. Adv. Mater.*, 2010, **2,** 413-420.

20 S. F. Xie, M. S. Jin, J. Tao, Y. C. Wang, Z. X. Xie, Y. M. Zhu and Y. N. Xia, *Chem. Eur. J.*, 2012, 18, 14974-14980.

21 (a) Z. Y.g Huo, C. K. Tsung, W. Y. Huang, X. F. Zhang and P. D. Yang, *Nano Lett.*, 2008, **8,** 2041-2044; (b) Z. G. Xiong, L. L. Zhang, J. Z. Ma and X. S. Zhao, *Chem. Commun.*, 2010, **46**, 6099-6101; (c) J. B. Zhao, H. Liu, S. Ye, Y. M. Cui, N. H. Xue, L. M. Peng, X. F. Guo and W. P. Ding, *Nanoscale*, 2013, **5**, 9546-9552.

22 P. N. Sisco and C. J. Murphy, *J. Phys. Chem. A,* 2009, **113**, 3973-3978.

23 L. Jiang, T. T. You, P. G. Yin, Y. Shang, D. F. Zhang, L. Guo and S. H. Yang, *Nanoscale*, 2013, **5,** 2784-2789.

24. Y. S. Li, H. M. Su, K. S. Wong and X. Y. Li, *J. Phys. Chem. C,* 2010, **114**, 10463-10477.

25 (a) M. I. Dar, S. Sampath and S. A. Shivashankar, *J. Mater. Chem.*, 2012, **22**, 22418-22423; (b) C. C. Kong, S. D. Sun, X. Z. Zhang, X. P. Song and Z. M. Yang, *CrystEngComm*, 2013, **15**, 6136-6139; (c) J. C. Santos Costa, R. A. Ando, A. C. Sant'Ana, L. M. Rossi, P. S. Santos, M. L. A. Temperini and P. Corio, *Phys. Chem. Chem. Phys.*, 2009, **11**, 7491-7498.

26 C. J. Orendorff, A. Gole, T. K. Sau and C. J. Murphy, *Anal. Chem.*, 2005, **77**, 3261-3266.

27 L. Osinkina, T. Lohmüller, F. Jäckel and J. Feldmann, *J. Phys. Chem. C,* 2013, **117**, 22198-22202.